

Modelling the ATP production in mitochondria

Alberto Saa · Kellen M. Siqueira

Received: date / Accepted: date

Abstract We revisit here the mathematical model for ATP production in mitochondria introduced recently by Bertram, Pedersen, Luciani, and Sherman (BPLS) as a simplification of the more complete but intricate Magnus and Keizer's model. We identify some inaccuracies in the BPLS original approximations for two flux rates, namely the adenine nucleotide translocator rate J_{ANT} and the calcium uniporter rate J_{uni} . We introduce new approximations for such flux rates and then analyze some of the dynamical properties of the model. We infer, from exhaustive numerical explorations, that the enhanced BPLS equations have a unique attractor fixed point for physiologically acceptable ranges of mitochondrial variables and respiration inputs, as one would indeed expect from homeostasis. We determine, in the stationary regime, the dependence of the mitochondrial variables on the respiration inputs, namely the cytosolic concentration of calcium Ca_c and the substrate fructose 1,6-bisphosphate FBP. The same dynamical effects of calcium and FBP saturations reported for the original BPLS model are observed here. We find out, however, a novel non-stationary effect which could be, in principle, physiologically interesting: some response times of the model tend to increase considerably for high concentrations of calcium and/or FBP. In particular, the larger the concentrations of Ca_c and/or FBP, the larger the necessary time to attain homeostasis.

Keywords Mitochondria · Calcium · ATP · Mathematical model

Alberto Saa
Departamento de Matemática Aplicada,
Universidade Estadual de Campinas,
13083-859 Campinas, SP, Brazil
E-mail: asaa@ime.unicamp.br

Kellen M. Siqueira
Instituto de Física "Gleb Wataghin",
Universidade Estadual de Campinas,
13083-859 Campinas, SP, Brazil
E-mail: kellenms@ifi.unicamp.br

1 Introduction

The exchange of energy in cells is mostly mediated by ATP (adenosine triphosphate) molecules. Such molecules are produced in several processes in an eukaryotic cell, but the principal source of ATP is typically the oxidative phosphorylation process which takes place in mitochondria. The mitochondrion is an organelle with two membranes, having, therefore, two distinct bulk regions: the intermembrane space and the mitochondrial matrix. In the inner membrane, there are plenty of protein transporters and ionic channels, some of which execute an active transport leading to a gradient of some ions and molecules [1,2]. The metabolic cascade that leads to the production of ATP in the mitochondrion starts in the cytoplasm. At first, glucose is transported from the extracellular medium into the cytoplasm by GLUT transporters. It is then converted in glucose-6-phosphate (G6P) by the enzyme hexokinase. G6P is then converted in pyruvate in a process called glycolysis, in which there is a net production of two ATP molecules. The pyruvate produced is transported into the mitochondrion (to the mitochondrial matrix) and is metabolized in a series of oxidation-reduction reactions in the citric acid cycle leading to the production of the nicotinamide adenine dinucleotide NAD and flavin adenine dinucleotide FAD. These electron donor molecules are oxidized in the complexes I to IV present in the inner mitochondrial membrane. These reactions lead to the activation of a proton pump, creating a pH gradient between the inter membrane space and the matrix. The protons pumped into the intermembrane space return to the matrix through a transporter that uses their energy to catalyze the conversion of ADP (adenosine diphosphate) into ATP. The ATP produced in the mitochondria is then transported to the cytoplasm by the ATP/ADP exchanger [1,2].

The kinetic aspects of the processes involved in the ATP production in mitochondria are rather intricate. This issue was addressed by Magnus and Keizer (MK), who introduced in the series of papers [3,4,5] a theoretical kinetic model for ATP production in mitochondria based on the known biophysical properties of the enzymes and transporters involved in the process. In fact, the MK model was built by considering electrical activity and cytosolic calcium handling in insulin-secreting pancreatic β -cells. The model consists basically in a set of equations describing the dynamics of the citric acid cycle, the proton pump, and the inner mitochondrial membrane transporters of ATP and calcium. The MK model is effectively based on first biophysical principles and provides a very detailed and accurate description of the processes considered to be important for mitochondrial oxidative phosphorylation. However, it is also a rather complex model with cumbersome equations, preventing a systematic mathematical study of its main dynamical and physiological properties.

A simplification of the MK model aiming to retain its main dynamical properties was introduced recently by Bertram, Pedersen, Luciani, and Sherman (BPLS) in [6]. The BPLS model incorporates some refinements introduced by Cortassa *et al.* in [7] for the description of the ATP production in cardiac cells. In fact, BPLS model can be considered as an approximation of the Cortassa *et*

al.'s model instead of the original MK one. As we will see, this was probably the origin of some inaccuracies in the BPLS equations. As in the original MK model, the mitochondrial ATP production in the BPLS model is governed by four dynamical variables, namely the potential drop in the inner membrane ΔV and the mitochondrial concentrations of: reduced nicotinamide adenine dinucleotide NADH, adenosine diphosphate ADP, and calcium Ca_m . The mitochondrial concentrations of pyridine and adenine nucleotides are assumed to be conserved

$$\text{NAD}_m + \text{NADH}_m = \text{NAD}_{\text{tot}}, \quad (1)$$

$$\text{ADP}_m + \text{ATP}_m = A_{\text{tot}}, \quad (2)$$

where NAD_{tot} and A_{tot} stand for the total mitochondrial concentration of the respective nucleotides. The balance of the pertinent fluxes and reactions yields to the following dynamical equations for the mitochondrial variables

$$\frac{d}{dt}\text{NADH} = J_{\text{PDH}} - J_0, \quad (3)$$

$$\frac{d}{dt}\text{ADP} = J_{\text{ANT}} - J_{\text{F1F0}}, \quad (4)$$

$$\frac{d}{dt}Ca_m = f_m (J_{\text{uni}} - J_{\text{NaCa}}), \quad (5)$$

$$\frac{d}{dt}\Delta V = C_m^{-1} (J_H - J_{\text{ANT}} - J_{\text{NaCa}} - 2J_{\text{uni}}), \quad (6)$$

where

$$J_H = J_{H,\text{res}} - J_{H,\text{ATP}} - J_{H,\text{leak}}. \quad (7)$$

The derivation and meaning of the fluxes presented in the right-handed sides of Eq. (3)-(6) are rather involved. The main details and the pertinent references can be found, for instance, in the BPLS paper [6]. We have checked carefully the derivation of each of these fluxes and we have found out some inaccuracies in the BPLS expressions for the adenine nucleotide translocator rate J_{ANT} and for the calcium uniporter rate J_{uni} . As we will see, some of these problems probably have originated in the transcription of the original MK equations to the Cortassa *et al.*'s model.

In the present paper, we propose some enhanced approximations in the BPLS framework for the fluxes J_{ANT} and J_{uni} and analyze some of the dynamical properties of Eqs. (3)-(6). We show, in particular, that for physiologically acceptable ranges of mitochondrial respiration inputs, namely the cytosolic concentration of calcium Ca_c and the substrate fructose 1,6-bisphosphate FBP, the BPLS equations have a unique physiologically acceptable attractor fixed point, as one would indeed expect for any model compatible with homeostasis. Exhaustive numerical explorations indicate that the BPLS model is indeed globally stable, reinforcing its relevance to physiological quantitative studies, despite its simplicity when compared to the MK original model. We determine, in the stationary regime, the dependence on constant respiration inputs Ca_c and FBP of the four mitochondrial variables considered in the model. As

in the original BPLS model, we observe here qualitatively distinct dynamical behavior for low and high concentrations of Ca_c and/or FBP. We detect, moreover, a non-stationary effect which could be, in principle, physiologically interesting: the inertia of the system tends to increase considerably for high concentrations of cytosolic calcium and FBP, *i.e.*, some response times of the model tend to increase considerably for high respiration inputs Ca_c and FBP. In particular, the larger the concentrations of Ca_c and/or FBP, the larger the necessary time to attain homeostasis.

2 The Enhanced BPLS Model

We will focus here in the problems we found for the BPLS expressions for the adenine nucleotide translocator rate J_{ANT} and for calcium uniporter rate J_{uni} , since all the other quantities appearing in (3)-(6) were checked to be correct and accurate for physiological ranges of variables and parameters. The MK expression for the former is (see Eq. (16) and Table 4 of [3])

$$J_{\text{ANT}} = V_{\text{max,ANT}} \frac{1 - \frac{\alpha_c}{\alpha_m} \frac{\text{ATP}_c}{\text{ADP}_c} \frac{\text{ADP}_m}{\text{ATP}_m} e^{-\frac{F\Delta V}{RT}}}{\left(1 + \alpha_c \frac{\text{ATP}_c}{\text{ADP}_c} e^{-f\frac{F\Delta V}{RT}}\right) \left(1 + \alpha_m^{-1} \frac{\text{ADP}_m}{\text{ATP}_m}\right)}. \quad (8)$$

The precise meaning of all the quantities presented in this formula can be found in [3, 4, 5], and in the BPLS paper [6] as well. (For the values of the parameters, see Table 1). On the other hand, the expression for J_{ANT} presented in the Eq. (35) of the Cortassa *et al.* paper [7] reads

$$J_{\text{ANT}} = V_{\text{max,ANT}} \frac{1 - \frac{\alpha_c}{\alpha_m} \frac{\text{ATP}_c}{\text{ADP}_c} \frac{\text{ADP}_m}{\text{ATP}_m}}{\left(1 + \alpha_c \frac{\text{ATP}_c}{\text{ADP}_c} e^{-f\frac{F\Delta V}{RT}}\right) \left(1 + \alpha_m^{-1} \frac{\text{ADP}_m}{\text{ATP}_m}\right)}. \quad (9)$$

By comparing with (8), we see clearly that it lacks the exponential in the numerator. Furthermore, the incorrect expression (9) is transcribed in the BPLS Eq. (35) as

$$J_{\text{ANT}} = V_{\text{max,ANT}} \frac{\frac{\text{ATP}_m}{\text{ADP}_m} - \frac{\alpha_c}{\alpha_m} \frac{\text{ATP}_c}{\text{ADP}_c}}{\left(1 + \alpha_c \frac{\text{ATP}_c}{\text{ADP}_c}\right) \left(\frac{\text{ATP}_m}{\text{ADP}_m} + \alpha_m^{-1}\right) e^{-f\frac{F\Delta V}{RT}}}, \quad (10)$$

i.e., with another mistake in the denominator. The BPLS expression for J_{ANT} , obtained from (10) after some simplifications, is

$$J_{\text{ANT}} = p_{19} \left(\frac{\frac{\text{ATP}_m}{\text{ADP}_m}}{\frac{\text{ATP}_m}{\text{ADP}_m} + p_{20}} \right) e^{f\frac{F\Delta V}{RT}}, \quad (11)$$

where p_{19} and p_{20} are some (fitted) numerical parameters. The (reasonable) physiological hypothesis used to derive (11) in the BPLS model is the assumption that, due to the ion transporters action, the rates of ATP to ADP in the

mitochondrial matrix and in the cytoplasm are approximately the same,

$$\frac{\text{ATP}_c}{\text{ADP}_c} \approx \frac{\text{ATP}_m}{\text{ADP}_m}. \quad (12)$$

Note that this assumption implies from (8) that $J_{\text{ANT}} \approx 0$ for $\text{ATP}_m \rightarrow \text{A}_{\text{tot}}$ (and, hence, $\text{ADP}_m \rightarrow 0$ according to (2)), which is incompatible with the BPLS expression (11). Another qualitatively different behavior arises for large values of ΔV : equation (8) implies that J_{ANT} tends to an asymptote, whereas (10) suggests an exponential growth. The expression (10) is clearly not accurate as an approximation of (8).

With the assumption (12) and taking into account the conservation of mitochondrial pyridine nucleotides (2), the original MK expression (8) for the adenine nucleotide translocator rate reads

$$J_{\text{ANT}} = V_{\text{max,ANT}} \left(\frac{\text{ATP}_m}{\text{A}_{\text{tot}} - (1 - \alpha_m)\text{ATP}_m} \right) \frac{\alpha_m - \alpha_c e^{-\frac{F\Delta V}{RT}}}{1 + \alpha_c \frac{\text{ATP}_m}{\text{A}_{\text{tot}} - \text{ATP}_m} e^{-f \frac{F\Delta V}{RT}}}. \quad (13)$$

This is our first proposed approximation, which captures all the essential properties of (8) and is still simple enough to be mathematically manipulated. Notice that for the typical range of physiological parameters, neglecting the exponential in the numerator of (13) would imply a relative error inferior to 5%. We will not, however, adopt this further approximation in this work. Figure (1) illustrate the discrepancies between the expressions (11) and (13) for typical physiological values of the parameters and variables. A closer inspection of the graphics (9) of [6] reveals that they have probably compared their approximated expression (11) with Eq. (10), which was itself transcribed incorrectly from Cortassa *et al.*'s Eq; (9).

With respect to the calcium uniporter rate J_{uni} , the original MK expression reads (see Eq. (19) in [3])

$$J_{\text{uni}} = V_{\text{max,uni}} \frac{\frac{2F}{RT}(\Delta V - \Delta V_0)}{1 - e^{-\frac{2F}{RT}(\Delta V - \Delta V_0)}} \left(\frac{\frac{\text{Ca}_c}{K_{\text{trans}}} \left(1 + \frac{\text{Ca}_c}{K_{\text{trans}}}\right)^3}{\left(1 + \frac{\text{Ca}_c}{K_{\text{trans}}}\right)^4 + \frac{L}{(1 + \text{Ca}_c/K_{\text{act}})^{n_a}}}} \right). \quad (14)$$

In the BPLS derivation of the approximation for J_{uni} , it is used Eq. (38) of Cortassa *et al.* [7], which reads

$$J_{\text{uni}} = V_{\text{max,uni}} \frac{\frac{\text{Ca}_c}{K_{\text{trans}}} \left(1 + \frac{\text{Ca}_c}{K_{\text{trans}}}\right)^3 \frac{2F}{RT}(\Delta V - \Delta V_0)}{\left(1 + \frac{\text{Ca}_c}{K_{\text{trans}}}\right)^4 + \frac{L}{(1 + \text{Ca}_c/K_{\text{act}})^{n_a}} \left(1 - e^{-\frac{2F}{RT}(\Delta V - \Delta V_0)}\right)}, \quad (15)$$

where one can see that there is a mistake in the denominator. The BPLS proposed expression for the calcium uniporter rate, obtained as a simplification of (15), is

$$J_{\text{uni}} = (p_{21}\Delta V - p_{22})\text{Ca}_c^2, \quad (16)$$

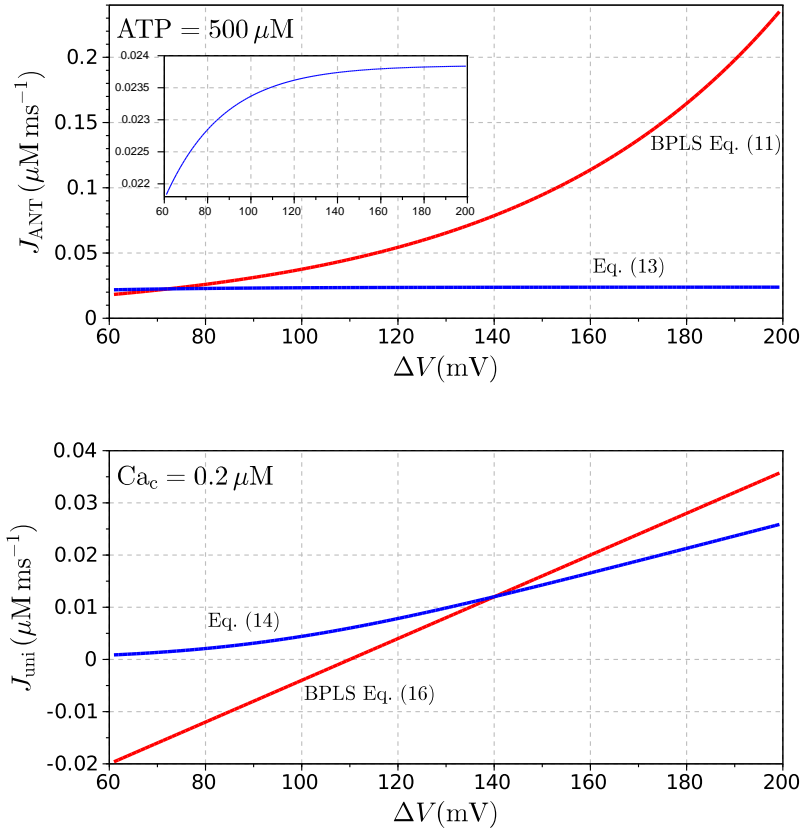


Fig. 1 Comparison between the original BPLS expressions and our proposals based on the original MK model. Above: The BPLS adenine nucleotide translocator rate J_{ANT} (11) and our proposal (13). We notice that the variation of (13) over physiological ranges (the inserted graphics) is considerably smaller than that one of (11). Furthermore, even the concavities of the curves are different. The dependency of (11) on ΔV is exponential, whereas (13) tends to an asymptote for large values of ΔV . In accordance to the Table 1, these curves were calculated by assuming $\text{ATP} = 500 \mu\text{M}$ and $\text{A}_{\text{tot}} = 15 \text{mM}$. Below: The BPLS calcium uniporter rate J_{uni} (16) and the original MK expression (14), both calculated for $\text{Ca}_c = 0.2 \mu\text{M}$. Eq. (16) is a straight line which implies non-positive rates for physiological values of ΔV .

where $p_{21} \approx 0.01 \mu\text{M}^{-1}\text{ms}^{-1}\text{mV}^{-1}$ and $p_{22} \approx 1.1 \mu\text{M}^{-1}\text{ms}^{-1}$ are also fitted numerical parameters. We found this equation to be inaccurate for the typical physiological range of parameters as well (see Figure (1)). Notice, in particular, that it implies in non-positive flux rates for $\Delta V \leq p_{22}/p_{21} \approx 110 \text{mV}$. We propose to keep in the approximated model the complete original MK equation (14). Its dependence on ΔV is already in a rather simple form, and the complications for Ca_c are harmless for the dynamical studies, as we will show.

For the dynamical analysis, it is more conveniently to introduce the following dimensionless variables

$$x = \frac{\text{NADH}_m}{\text{NAD}_{\text{tot}}}, \quad (17)$$

$$y = \frac{\text{ATP}_m}{\text{A}_{\text{tot}}}, \quad (18)$$

$$z = \frac{\text{Ca}_m}{\text{Ca}_0}, \quad (19)$$

$$w = \frac{\Delta V}{\Delta V_0}, \quad (20)$$

$$u = \frac{\text{Ca}_c}{\text{Ca}_0}, \quad (21)$$

$$v = \frac{\text{FBP}}{\text{FBP}_0}, \quad (22)$$

Taking into account the new proposed expressions (13) and (14), the rates in the right-handed sides of (3)-(6) will be given by

$$J_{\text{PDH}} = r_1 \sqrt{v} \frac{z}{a_1 + z} \left(a_2 + \frac{x}{1-x} \right)^{-1}, \quad (23)$$

$$J_0 = r_2 \frac{x}{a_3 + x} (1 + a_4 e^{a_5 w})^{-1}, \quad (24)$$

$$J_{\text{ANT}} = r_3 \left(\frac{y}{1 - a_6 y} \right) \frac{a_7 - a_8 e^{-a_9 w}}{1 + a_8 \frac{y}{1-y} e^{-a_{10} w}}, \quad (25)$$

$$J_{F_1F_0} = r_4 [(a_{11} + y) (1 + a_{12} e^{-a_{13} w})]^{-1}, \quad (26)$$

$$J_{H,\text{res}} = a_{14} J_0, \quad (27)$$

$$J_{H,\text{ATP}} = a_{15} J_{F_1F_0}, \quad (28)$$

$$J_{H,\text{leak}} = r_5 (w - a_{16}), \quad (29)$$

$$J_{\text{NaCa}} = r_6 \frac{z}{u} e^{a_{17} w}, \quad (30)$$

$$J_{\text{uni}} = r_7 \frac{a_{18}(w-1)}{1 - e^{-a_{18}(w-1)}} G(u), \quad (31)$$

where

$$G(u) = \frac{u(1 + a_{19}u)^{n_a}(1 + a_{20}u)^3}{a_{21} + (1 + a_{19}u)^{n_a}(1 + a_{20}u)^4}. \quad (32)$$

All the values of the numerical parameters and constants are presented in Table 1. With the new dimensionless variables, the Eqs. (3)-(6) can be cast in the form

$$\dot{x} = \frac{1}{\text{NAD}_{\text{tot}}} (J_{\text{PDH}} - J_0), \quad (33)$$

$$\dot{y} = \frac{1}{\text{A}_{\text{tot}}} (J_{F_1F_0} - J_{\text{ANT}}), \quad (34)$$

$\text{NAD}_{\text{tot}} = 10 \times 10^3 \mu\text{M}$	$A_{\text{tot}} = 15 \times 10^3 \mu\text{M}$	$\text{Ca}_0 = 0.2 \mu\text{M}$
$\Delta V_0 = 91 \text{ mV}$	$\text{FBP}_0 = 1 \mu\text{M}$	$C_m = 1.8 \mu\text{M mV}^{-1}$
$V_{\text{max,ANT}} = 5 \mu\text{M ms}^{-1}$	$V_{\text{max,uni}} = 10 \mu\text{M ms}^{-1}$	$\frac{F}{RT} = 0.037 \text{ mV}^{-1}$
$f = 0.5$	$K_{\text{trans}} = 19 \mu\text{M}$	$K_{\text{act}} = 0.38 \mu\text{M}$
$L = 110$	$f_m = 0.01$	$n_a = 2.8$
$\alpha_c = 0.111$	$\alpha_m = 0.139$	
$r_1 = 0.2 \mu\text{M ms}^{-1}$	$r_2 = 0.6 \mu\text{M ms}^{-1}$	$r_3 = 5 \mu\text{M ms}^{-1}$
$r_4 = 23.3 \mu\text{M ms}^{-1}$	$r_5 = 0.182 \mu\text{M ms}^{-1}$	$r_6 = 0.001 \mu\text{M ms}^{-1}$
$r_7 = 0.11 \mu\text{M ms}^{-1}$		
$a_1 = 0.05$	$a_2 = 1$	$a_3 = 0.01$
$a_4 = 4.23 \times 10^{-16}$	$a_5 = 18.2$	$a_6 = 0.861$
$a_7 = 0.139$	$a_8 = 0.111$	$a_9 = 3.37$
$a_{10} = 1.68$	$a_{11} = 0.67$	$a_{12} = 5.10 \times 10^9$
$a_{13} = 10.7$	$a_{14} = 11.7$	$a_{15} = 3.43$
$a_{16} = 0.16$	$a_{17} = 1.46$	$a_{18} = 6.73$
$a_{19} = 0.52$	$a_{20} = 0.01$	$a_{21} = 110$

Table 1 Numerical parameters and rates for the enhanced BPLS model, see equations (17)-(36). All the values were obtained from [3, 4, 5] and [6].

$$\dot{z} = \frac{f_m}{\text{Ca}_0} (J_{\text{uni}} - J_{\text{NaCa}}), \quad (35)$$

$$\dot{w} = \frac{1}{C_m \Delta V_0} (J_H - J_{\text{ANT}} - J_{\text{NaCa}} - 2J_{\text{uni}}), \quad (36)$$

where f_m and C_m stand, respectively, for the fraction of free Ca ions and the mitochondrial capacitance, see Table 1. Equations (33)-(36) form a non-autonomous systems of four first order differential equations. The external excitations $u(t)$ and $v(t)$ are related, respectively, to the cytosolic concentration of calcium Ca_c and the substrate fructose 1,6-bisphosphate FBP, see Eqs. (21) and (22). We can now start the dynamical analysis of the model.

3 Dynamics of the model

Let us consider initially the fixed points (x_*, y_*, z_*, w_*) of the system (33)-(36) assuming constant inputs (u_*, v_*) . By construction, the physiologically meaningful range for the variables x and y is $[0, 1]$, see (1)-(2) and (17)-(18). For z and w , we assume only that they are non negative. The typical physiological range for the potential drop, however, is more restrictive, corresponding to $\Delta V \approx [90, 225] \text{ mV}$, which is equivalent to $w \approx [1, 2.5]$. For the inputs u and v , we consider the ranges $[0, 10]$ and $[0, 20]$, respectively, which corresponds to $\text{Ca}_c \approx [0, 2] \mu\text{M}$ and $\text{FBP} \approx [0, 20] \mu\text{M}$. We perform an exhaustive numerical search [8] for fixed points of (33)-(36) by assuming $u \in [0, 10]$ and $v \in [0, 20]$ constants. For all tested values of u and v , only one physiological ($x, y \in [0, 1]$ both $z, w > 0$) fixed point was found, which is always stable. Moreover, the fixed point is globally stable for physiological ranges of variables, meaning that any solution of (33)-(36) with reasonable initial conditions will tend asymptotically to the fixed point, *i.e.*, the system indeed exhibits an asymptotic behavior

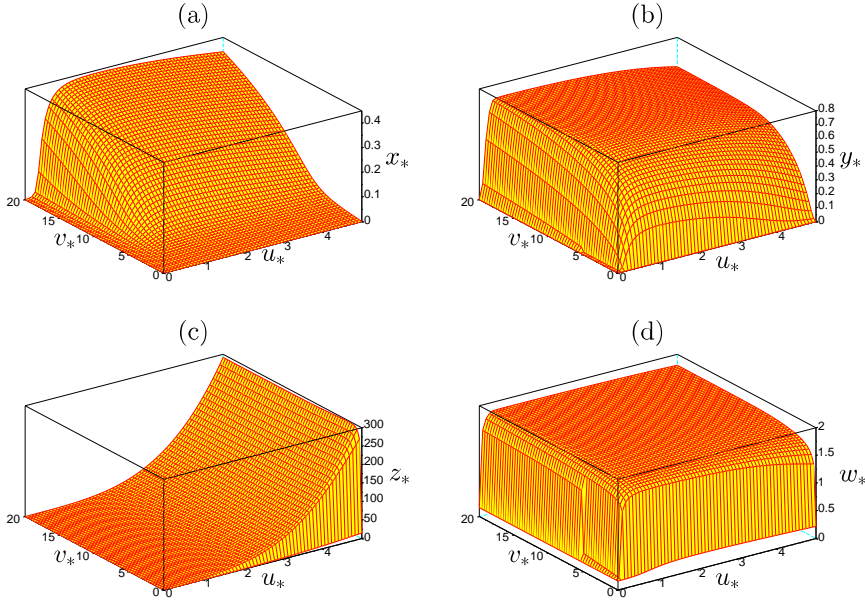


Fig. 2 The globally stable physiological fixed point (x_*, y_*, z_*, w_*) of the system (33)-(36) assuming constant inputs (u_*, v_*) .

compatible with homeostasis. Starting at a random point in the phase space, the variables w and x have typically the quickest convergence to the fixed point, where y and z are the slowest ones. The values of (x_*, y_*, z_*, w_*) as function of the constant inputs (u_*, v_*) are depicted in Fig. (2), from where one can already observe some physiologically consistent dynamical properties which we describe in detail below.

The first observations is that the production of ATP and the concentration of NADH vanishes in the absence of cytosolic calcium Ca_c and/or the substrate fructose 1,6-bisphosphate FBP, *i.e.*, x_* and $y_* \rightarrow 0$ for u_* or $v_* \rightarrow 0$. Notice that, from the condition $J_{\text{NaCa}} = J_{\text{uni}}$ defining the fixed point $\dot{z}_* = 0$ (see Eq. (35)), we have $z_* = 0$ for $u_* = 0$. On the other hand, J_{PDH} vanishes for $z_* = 0$ (and for $v_* = 0$ as well), which implies via the condition $\dot{x}_* = 0$ that $J_0 = 0$ and, consequently, $x_* = 0$. The condition for y_* and w_* are more involved. The former vanishes for vanishing u_* or v_* , while the latter will be given by $w_* \approx a_{16} = 0.16$ for $u_* = 0$. Also, we see that for reasonable values of u_* and v_* the value of the potential drop $\Delta V (w_*)$ is almost constant and close to 150 mV ($w_* = 1.65$). This stability is probably the reason why the original BPLS model is robust, despite the inaccuracies for the expression of J_{ANT} and J_{uni} we are correcting in this paper. We will return to this point in the last section. Still from the condition $J_{\text{NaCa}} = J_{\text{uni}}$, we see that $z_* \propto u_* G(u_*)$, since w_* is almost constant for physiological reasonable values of u_* and v_* (see Fig. (2c)).

Another important feature of the BPLS model is the reversion of the dynamical behavior of some mitochondrial variables in the presence of lower and higher concentration of cytosolic calcium and FBP. This behavior can be seen, for instance, in Fig. (2b). After attaining its maximum, the ATP production (y_*) tends to decrease for increasing cytosolic calcium concentrations (u_*). Calcium saturation can be simulated, as described in [6], by setting $a_1 = 0$ in the expression for J_{PDH} (23). The reversion of the dynamical behavior of the other mitochondrial variables for higher Ca_c concentrations can also be inferred directly from Fig. 2, but it is certainly better illustrated in Fig. 3, which depicts the solutions of (33)-(36) for an oscillatory Ca_c input of the form

$$u(t) = u_0 + u_1 \sin(t/t_0), \quad (37)$$

with constant $v(t)$ and initial conditions $(x(0), y(0), z(0), w(0))$ given by the values of the fixed point corresponding to $u_* = u(0)$ and $v_* = v(0)$. As we will see, such a choice of initial condition is consistent with the adiabatic (stationary) regime we observe for sufficiently slow inputs (large periods t_0). For lower values of u_0 (low Ca_c concentrations), all the mitochondrial variables increases and decreases in synchrony with the variations of u . On the other hand, for higher values of u_0 , the dynamical behavior of x , y and w is reversed. *i.e.*, they tend to decrease/increase while u increases/decreases. This effect can be understood from the relation between u_* and z_* depicted in Fig. (2c). The value of z_* tends to increase rapidly when u_* increases and, for large values of z , the dependence of the expression for J_{PDH} (23) on z saturates and becomes equivalent to setting $a_1 = 0$. Without the z suppression term in J_{PDH} , the dynamical behavior of the variables x , y , and w is reversed, as it was pointed out in the original BPLS analysis. Low variations of v (FBP) do not change qualitatively this dynamical behavior. However, the situation changes for large concentrations of FBP. As described in [6], for low concentrations of FBP, the NADH_m concentration reacts to a sudden rising of Ca_c with an upward teeth, while for high concentrations of FBP such behavior is reversed, *i.e.*, NADH_m concentration exhibits a downward teeth if Ca_c increases. This situation is analyzed and depicted in Fig. (4).

The oscillatory excitations used in the examples depicted in Fig. (3) and (4) have period $t_0 = 3$ min. For inputs varying over a time scale of minutes, the system evolves adiabatically in a good approximation, *i.e.*, the instantaneous solution $(x(t), y(t), z(t), w(t))$ is well approximated by the fixed point (x_*, y_*, z_*, w_*) corresponding to $u_* = u(t)$ and $v_* = v(t)$. In other words, for slowly varying inputs, the solutions of the system are confined to the fixed-point surfaces depicted in Fig. 2. Of course, one expects a breakdown of this adiabatic behavior for rapidly varying inputs. Non-stationary effects must appear for inputs varying with a characteristic time smaller than a certain critical value. In order to study non-stationary effects in our model, we consider the response of the system for inputs of the type

$$u(t) = u_0 + u_1 \tanh\left(\frac{t - t_1}{t_0}\right), \quad (38)$$

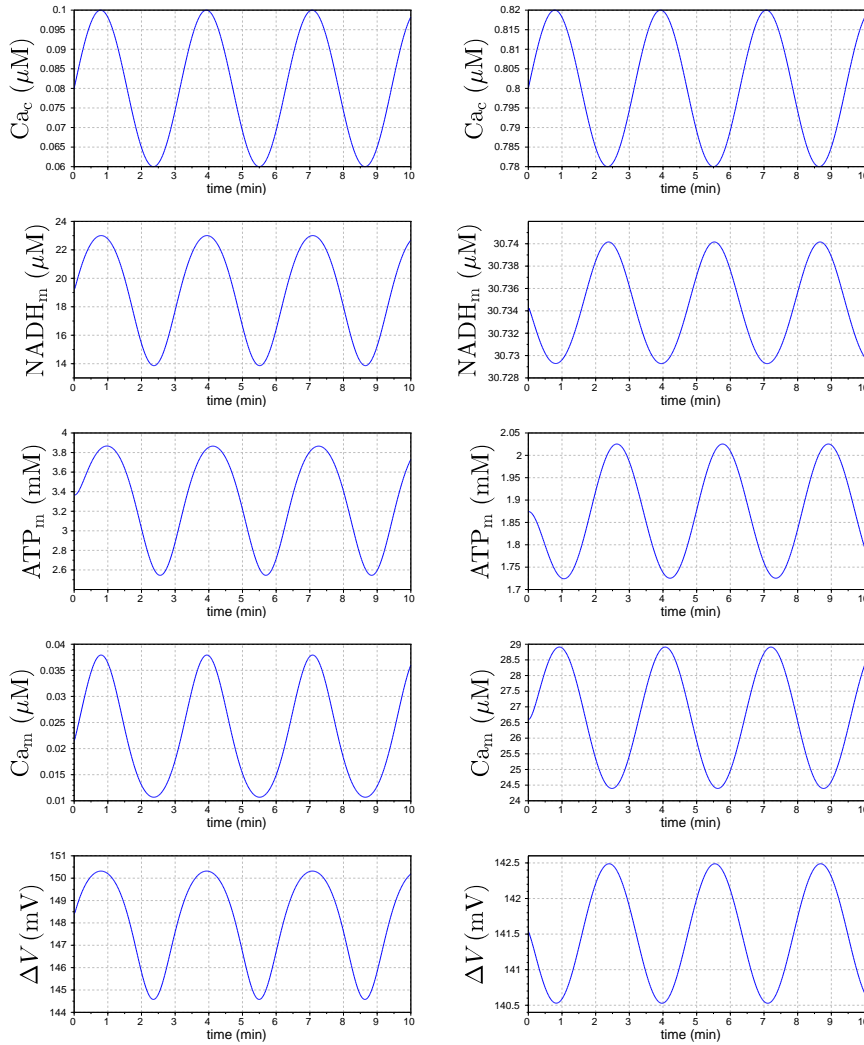


Fig. 3 Response of the equations (33)-(36) to oscillatory inputs (37). Notice that for low Ca_c concentrations (left), all the mitochondrial variables increases and decreases in synchrony with the variations of u . On the other hand, for high Ca_c concentrations (right), the behavior of x , y and w is reversed. All the curves were evaluated for $FBP = 0.5 \mu\text{M}$. See the text for further details.

for different values of t_0 . This situation is depicted in Fig. 5 for some values of u_0 and u_1 and for $t_0 = 2.5, 1, 0.5$, and 0.02 seconds. It is clear that for lower values of u (Ca_c), approximately 10 seconds are enough to assure that $NADH_m$ concentration and ΔV reaches their values corresponding to the adiabatic regime, which in this case corresponds to the homeostasis. As we have already noticed, the variables y (ATP) and z (Ca_m) are the slowest ones to attain their respective stationary regimes. For lower values of $f u$ (Ca_c), they spend

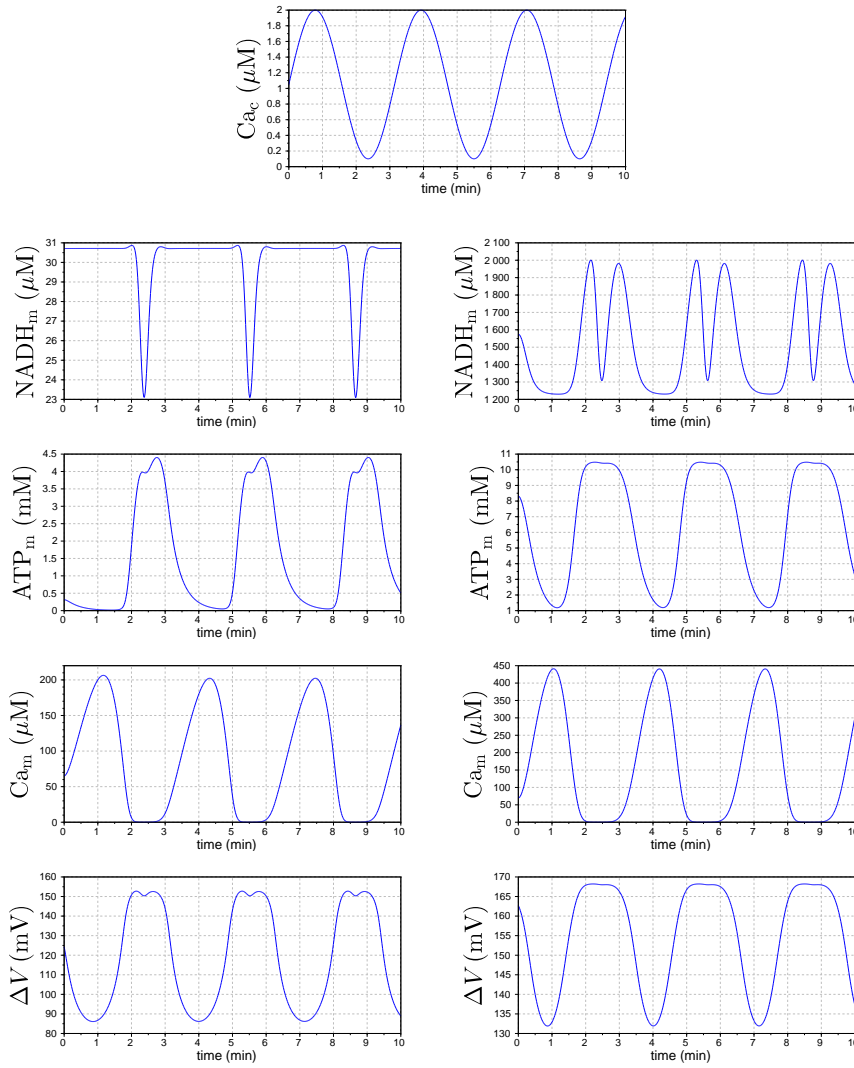


Fig. 4 Response of the equations (33)-(36) to oscillatory inputs (37) for different concentrations of FBP. The system is submitted to the oscillatory input corresponding to the top graphic. The left column is the response for $\text{FBP} = 0.5 \mu\text{M}$, while the right one corresponds to $\text{FBP} = 10 \mu\text{M}$. It's clear that the NADH_m concentration reverses its dynamical behavior for low and high concentrations of FBP. See the text for further details.

approximately 40 seconds to stabilize. Increasing the values of u implies the increasing of such “relaxation” times, *i.e.*, a larger time is necessary to attain homeostasis. The second column in Fig. 5 corresponds to a situation with $u \in [2, 4]$, for which almost 30 seconds are necessary to assure the attainment of the stationary regime for the rapid variable w , whereas the slow one will

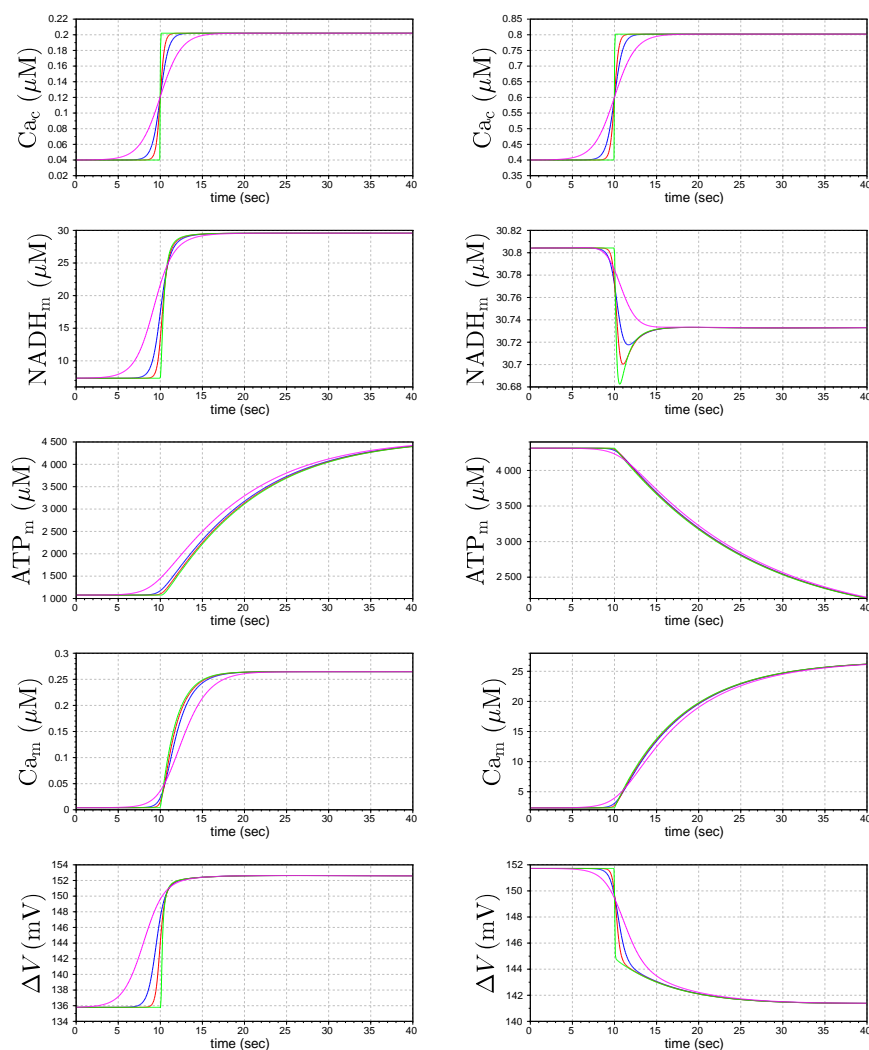


Fig. 5 Response of the equations (33)-(36) to step-like inputs (38). The magenta, blue, red, and green curves correspond, respectively, to $t_0 = 2.5, 1, 0.5,$ and 0.02 seconds. The inertia of the system increases considerably for higher values of u , see the text for further details. The curves were evaluated for $\text{FBP} = 0.5 \mu\text{M}$.

need a few minutes. The inertia of the system, hence, increases considerably for higher concentrations of cytosolic calcium.

Higher concentrations of fructose 1,6-bisphosphate FBP also imply an increasing of the inertia of the system. This situation is analyzed and depicted in Fig. (6). Besides the increasing of the relaxation times, for higher concentrations of FBP we observe a smoothing out of the dynamical response of NADH_m . In particular, its overshooting present for large variations of CA_c

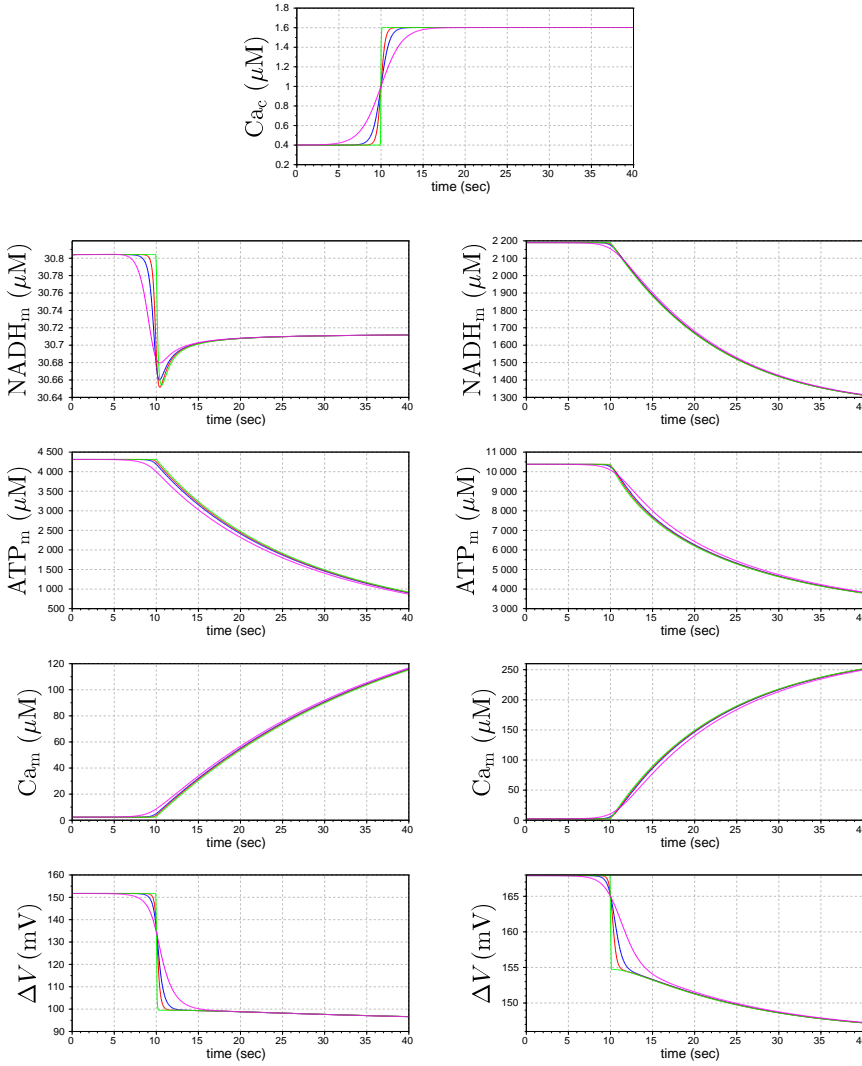


Fig. 6 Response of the equations (33)-(36) to step-like inputs (38). The magenta, blue, red, and green curves correspond, respectively, to $t_0 = 2.5, 1, 0.5,$ and 0.02 seconds. The inertia of the system also increases considerably for higher values of v , see the text for further details. The system is submitted to the input corresponding to the top graphics. The left column depicts the response for $\text{FBP} = 0.5 \mu\text{M}$, while the right one corresponds to $\text{FBP} = 10 \mu\text{M}$. See the text for further details.

and low FBP disappears for the high FBP concentration case, compare Figures (5) and (6). By examining this overshooting in the dynamics of NADH_m , our rapidest variable, it is possible to estimate the critical time for which any adiabatic approximation should break. We can see from Figures (5) and (6) that the overshooting appears for transitions occurring in less than 2.5 seconds

approximately. We do not expect any stationary response for input variables varying over periods smaller than this.

4 Final Remarks

We have revisited here the mathematical model for ATP production in mitochondria introduced recently by Bertram, Pedersen, Luciani, and Sherman (BPLS) in [6] as a simplification of the more complete but intricate Magnus and Keizer's model [3, 4, 5]. We checked carefully all the approximations introduced in the BPLS model and found some inaccuracies for the approximations used for the adenine nucleotide translocator rate J_{ANT} and for the calcium uniporter rate J_{uni} . We proposed some enhanced approximations for such rates based on the original Magnus and Keizer's model and analyzed some dynamical properties of the model. Our results for the stationary regime indicate that the BPLS model is indeed globally stable, reinforcing its relevance to physiological quantitative studies, despite its simplicity when compared to the Magnus and Keizer's model. We have considered also the non-stationary regime and detected an effect which could be, in principle, physiologically interesting: the inertia of the system tends to increase considerably for high concentrations of cytosolic calcium and FBP, *i.e.*, some response times of the model tend to increase considerably for high respiration inputs Ca_c and FBP. In particular, for $\text{Ca}_c \approx 0.2 \mu\text{M}$ and $\text{FBP} \approx 0.5 \mu\text{M}$, approximately 10 seconds are necessary to NADH_m and ΔV attain homeostasis after a sudden increasing in Ca_c . The variables ATP_m and Ca_m are typically slower and need approximately 30 seconds to attain homeostasis in the same conditions. Keeping FBP constant and increasing Ca_c , or keeping Ca_c and increasing FBP, will imply a considerably increasing of this response time, *i.e.*, the system will take a longer time to attain homeostasis.

It is interesting to notice that the dynamics of our enhanced model are qualitatively similar to the original BPLS one, despite the differences in the rates J_{ANT} and J_{uni} for physiological ranges, as depicted, for instance, in Fig. 1. This point can be understood from the fact that the value of w_* , which does not depend tightly on the details of such rates, is almost constant and corresponding to $\Delta V = 150 \text{ mV}$ for reasonable values of the inputs v_* and u_* . For a fixed value of ΔV , the numerical parameters in (11) can be fitted to provide a good adjustment for the real ATP dependence of (13). An inspection of Fig. 9 of [6] reveals that the adjustment of their numerical parameters was probably checked for $\text{ATP} \approx 3 \text{ mM}$ and for $\Delta V \approx 160 \text{ mV}$, which is close to the physiological global fixed point (homeostasis), explaining why the asymptotic dynamics are not strongly affected by the inaccuracies in the BPLS approximations. On the other hand, we do not expect that the detected non-stationary effects be independent on the details of J_{ANT} and J_{uni} . Such points certainly deserve further investigations.

Acknowledgements The authors are grateful to FAPESP and CNPq for the financial support. AS wishes to thank Prof. Leon Brenig for the warm hospitality at the Brussels Free University, where part of this work was carried on.

References

1. A. C. Guyton and J. E. Hall, Textbook of Medical Physiology, Elsevier (2006).
2. D. L. Nelson and M. Cox, Lehninger Principles of Biochemistry, W. H. Freeman and Company (2004).
3. G. Magnus and J. Keizer, Am. J. Physiol. **273**, C717-C733 (1997).
4. G. Magnus and J. Keizer, Am. J. Physiol. **274**, C1158-C1173 (1998).
5. G. Magnus and J. Keizer, Am. J. Physiol. **274**, C1174-C1184 (1998).
6. R. Bertram, M.G. Pedersen, D.S. Luciani, and A. Shermant, J. Theor. Biol. **243**, 575-586 (2006).
7. S. Cortassa, M.A. Aon, E. Marban, R.L. Winslow, and B. O'Rourke, Biophys. J. **84**, 2734-2755 (2003).
8. Scilab files are available at <http://vigo.ime.unicamp.br/atp>